Epitaxial Graphene Materials Integration: Effects of Dielectric Overlayers on Structural and Electronic Properties

Joshua A. Robinson,[†,‡,*] Michael LaBella III,[†] Kathleen A. Trumbull,[†] Xiaojun Weng,[§] Randall Cavelero,[†] Tad Daniels,[§] Zachary Hughes,[†] Mathew Hollander,[†,‡] Mark Fanton,[†] and David Snyder[†,⊥]

[†]The Electro-Optics Center, [‡]Department of Materials Science and Engineering, [§]Materials Research Institute, and [⊥]Department of Chemical Engineering, The Pennsylvania State University, University Park, Pennsylvania 16802

ABSTRACT We present the integration of epitaxial graphene with thin film dielectric materials for the purpose of graphene transistor development. The impact on epitaxial graphene structural and electronic properties following deposition of Al_2O_3, HfO_2, TiO_2, and Ta_2O_5 varies based on the choice of dielectric and deposition parameters. Each dielectric film requires the use of a nucleation layer to ensure uniform, continuous coverage on the graphene surface. Graphene quality degrades most severely following deposition of Ta_2O_5, while the deposition if TiO_2 appears to improve the graphene carrier mobility. Finally, we discuss the potential of dielectric stack engineering for improved transistor performance.

KEYWORDS: graphene · epitaxial graphene · gate oxide · atomic layer deposition · Al_2O_3 · HfO_2 · TiO_2 · Ta_2O_5

The realization of a graphene-based electronic technology necessitates large-area graphene production, as well as the ability to integrate graphene with highly insulating films that act as the gate dielectric in field-effect transistors (FETs). Interest in dielectric materials with high permittivity values (high-*k* dielectrics) originates from the aggressive scaling of traditional silicon transistors which produce unacceptably high leakage currents in the silicon dioxide (SiO_2) gate oxide.[1,2] As a result, high-*k* dielectric materials such as hafnium oxide (HfO_2, permittivity (ε_r) = 25), aluminum oxide (Al_2O_3, $\varepsilon_r = 9$), tantalum oxide (Ta_2O_5, $\varepsilon_r = 25$), and titanium oxide (TiO_2, $\varepsilon_r = 80$) have been explored.[1,2] The use of high-*k* dielectric materials in graphene-based FETs is also of interest because of the reduced Coulombic scattering of charge carriers[3,4] and enhanced charge carrier mobility.[5] Although the use of high-*k* dielectric materials may limit graphene mobility through phonon scattering,[6,7] graphene FETs fabricated with high-*k* dielectric materials still outperform those utilizing SiO_2.[8−10] In this article, we present a means to integrate the high-*k* dielectric materials Al_2O_3, HfO_2, Ta_2O_5, and TiO_2 with epitaxial graphene grown on the silicon face of silicon carbide (SiC(0001)), compare surface pretreatments, and provide electronic and structural characterization of the dielectric materials on graphene. We present evidence that, by providing the proper nucleation layer, atomic layer deposition of high-*k* dielectrics may improve the mobility of epitaxial graphene by up to 22%. Finally, we discuss the use of multilayer films that provide uniform coverage and minimal degradation of epitaxial graphene's electronic and structural properties.

Thermal atomic layer deposition (ALD) provides a means to produce high-quality films for gate dielectrics at temperatures below 300 °C and has proven to be an excellent technique toward the integration of dielectrics with graphene.[10,11] However, because this type of ALD is a water-based technique, graphene must undergo surface preparation processes that will permit the deposition of a uniform dielectric film. Previous reports suggest that functionalization of graphene *via* ozone,[12] nitrogen dioxide,[13] or perylene tetracarboxylic acid (PTCA)[14] prior to ALD of Al_2O_3 can result in more uniform dielectric film coverage on graphene, with fewer examples of uniform deposition on pristine graphene.[15] Additionally, Farmer *et al.*[11] introduced the use of a low-*k* polymer on the surface of graphene prior to deposition of HfO_2 to achieve uniform coverage on exfoliated graphene. Finally, successful integration of Al_2O_3 and HfO_2 has been accomplished by depositing a thin

*Address correspondence to jrobinson@psu.edu.

Received for review February 16, 2010 and accepted April 19, 2010.

Published online April 23, 2010.
10.1021/nn1003138

(2−5 nm) metallic Al or Hf film *via* physical vapor deposition, which fully oxidized when exposed to atmosphere and served as a uniform nucleation layer for subsequent ALD processing.[10,16] We find that this last method is highly reproducible and have adopted it as the seeding method in the current work.

RESULTS AND DISCUSSION

Uniform coverage of ALD dielectric films on epitaxial graphene is possible through the use of a nucleation layer and optimization of deposition temperature. Our initial work focused on the deposition of oxides on few-layer epitaxial graphene at temperatures <100 °C without a nucleation layer. While the use of a nucleation layer may not be required for HfO_2 films ≥25 nm,[17] successful deposition of continuous HfO_2 films benefits greatly by increasing the deposition temperature from 80 °C (Figure 1a) to 110 °C (Figure 1b). We must note, however, that the deposition of thin HfO_2 films (≤20 nm), such as that presented in Figure 1b, does not result in a uniform, continuous film.[11,18] Further increase of the deposition temperature to 250 °C (Figure 1c) leads to the growth of a discontinuous HfO_2 layer on the graphene surface. Additionally, Raman spectroscopy and TEM indicate that the graphene has been etched away in those regions where HfO_2 is not present in Figure 1c. While the true mechanism of graphene removal is not well understood, we speculate that it may result from an unwanted reaction with H_2O or the Hf precursor at elevated temperatures. Deposition of Al_2O_3, Ta_2O_5, and TiO_2 also results in non-uniform coverage up to the maximum deposition temperature of our system (300 °C) without the presence of a nucleation layer on the graphene surface.[28] Figure 2 illustrates the evolution of film coverage, uniformity, and roughness when a seed layer is present for seeded Al_2O_3 (Figure 2a,b), TiO_2 (Figure 2c,d), and Ta_2O_5 (Figure 2e,f). Film uniformity and coverage significantly improve for Al_2O_3 as the temperature is increased from 150 °C (Figure 2a) to 300 °C (Figure 2b), with film particulate size decreasing from an average of 50 nm to less than 10 nm. Additionally, according to Raman spectroscopy, there is no apparent increase in the defect density (measured by the ratio of the D and G peak) for films deposited at 300 °C, indicating that the oxidized Al nucleation layer may protect the underlying graphene during high-temperature ALD depositions. Deposition of TiO_2 on graphene with a Ti seed layer results in films that are conformal and continuous at both 120 °C (Figure 2c) and 250 °C (Figure 2d). Finally, deposition of Ta_2O_5 on graphene with a Ta nucleation layer results in a poor film morphology regardless of temperature. Despite the uniform deposition of a Ta nucleation layer,[28] ALD deposition of Ta_2O_5 results in large particulates and film buckling with peak-to-valley measurements greater than 50 nm. Surface morphology alone does not yield direct evidence of how ALD affects the underlying graphene structure; however, without further optimization, it indicates that the use of Ta_2O_5 as a gate dielectric may result in poor transistor performance.

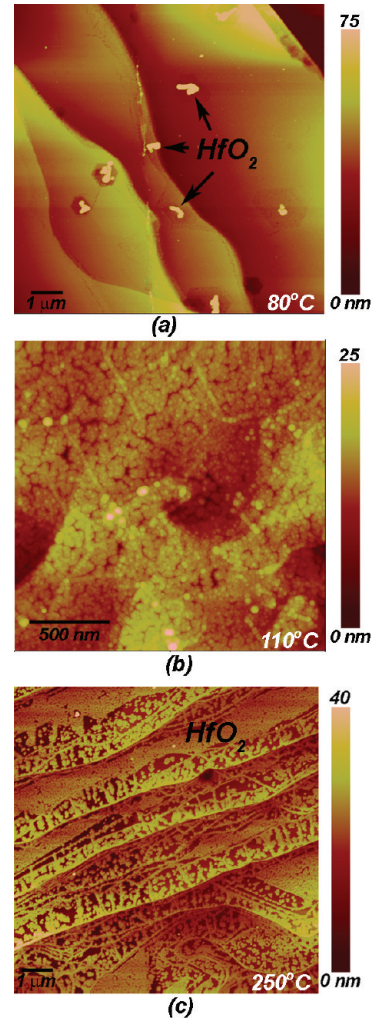

Figure 1. Atomic force microscopy of HfO_2 films deposited on epitaxial graphene at 80 °C (a), 110 °C (b), and 250 °C (c). Island formation of HfO_2 occurs at low temperature, while complete coverage is accomplished at 110 °C. The coverage at 110 °C, however, is accompanied by a high density of cracks and pits in the film due to incomplete coalescence of the film. Increasing the deposition temperature to 250 °C results in a dendrite-like growth of HfO_2 on the graphene surface, accompanied by significant degradation of the graphene film.

Deposition of dielectric materials *via* ALD impacts the structural quality of epitaxial graphene. Graphene structure is often qualified *via* the comparison of the D (1360 cm^{-1}) and G (1590 cm^{-1}) peak in Raman spectroscopy.[19] Graphene grown in the current study exhibits a Raman D/G peak ratio of 0.04−0.10, corresponding to an approximate crystallite size range of 140−340 nm.[19] Subsequent processing *via* the deposition of nucleation layers and ALD of dielectric materials generally results in an increase of the D/G ratio to >0.1, with ratios as high as 0.3 in the case of Ta_2O_5 (Table 1). Figure 3 presents TEM micrographs with corresponding Raman spectra of the graphene D and G peak (Figure 3e)

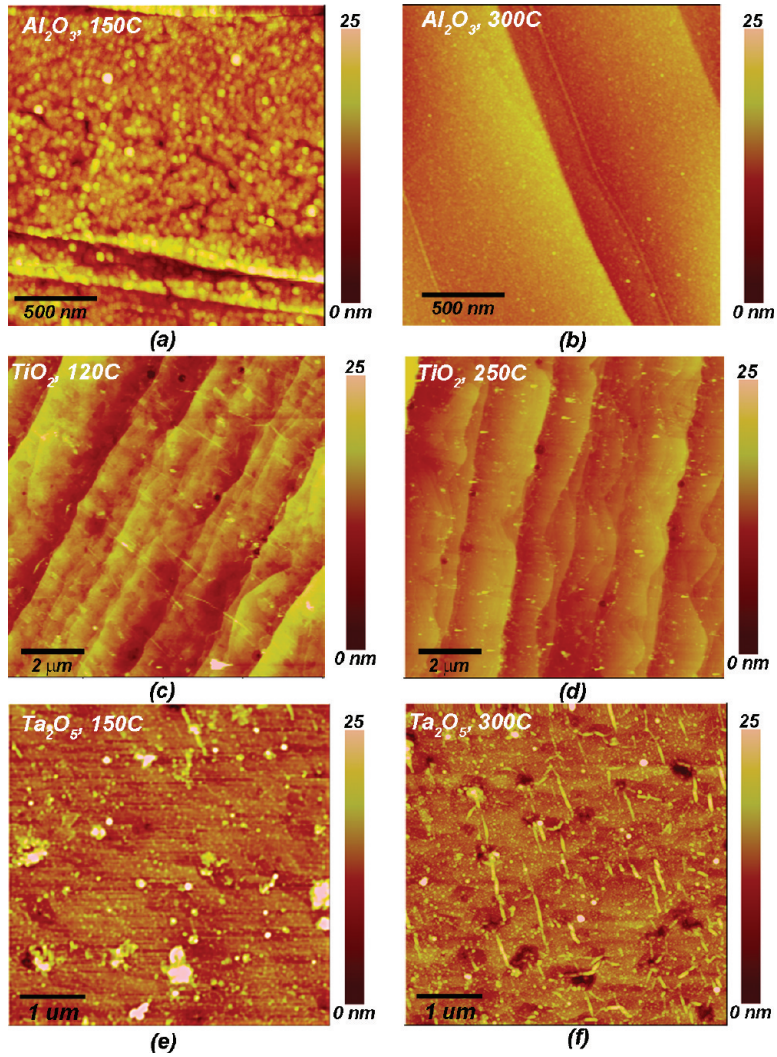

Figure 2. Film uniformity and coverage on seeded graphene is dependent on deposition temperature. Atomic force microscopy of seeded Al_2O_3, TiO_2, Ta_2O_5. Films deposited on graphene *via* ALD indicates that Al_2O_3 requires temperatures >150 °C while complete coverage of TiO_2 and Ta_2O_5 occurs at ≤150 °C. The use of Ta_2O_5 as a dielectric material, however, may result in an unacceptable surface roughness for subsequent device fabrication.

for Al_2O_3 deposited on an Al-seeded graphene film at 300 °C (Figure 3a), HfO_2 deposited on pristine graphene at 110 °C (Figure 3b), TiO_2 deposited on a Ti-seeded graphene film at 250 °C (Figure 3c), and Ta_2O_5 deposited on a Ta-seeded graphene film at 150 °C (Figure 3d). According to TEM, the deposition of Al_2O_3 and HfO_2 results in an interface consisting of a high density of defects. Averaging 100 Raman spectra confirms a slight increase in the D/G ratio for Al_2O_3 (Table 1) following ALD processing. Similarly, the deposition of TiO_2 appears to result in the degradation of the top layer of the epitaxial graphene. However, according to Raman studies (Figure 3e and Table 1), no significant change in the D/G peak ratio can be measured for TiO_2 compared to as-grown material. Finally, the deposition of Ta_2O_5 on Ta-seeded graphene results in considerable degradation of the graphene (Figure 3d), with all but the very bottom layer of graphene being completely destroyed. Direct comparison of representative Raman spectra indicates that Al_2O_3, HfO_2, and TiO_2 have little impact on the structural integrity of graphene; however, TEM presents evidence that the top layer of all graphene films exhibits defect densities much higher than underlying layers. While both techniques do suggest an increase in defects as a result of the ALD process, Raman spectroscopy indicates that the level of defectiveness in as-grown graphene is very near that of processed graphene. We have also observed similar defect levels in the top layer of graphene grown on SiC(0001) *via* TEM;[20] however, the defects were thought to have occurred during TEM sample preparation. Given that the graphene is protected during TEM preparation when a dielectric overlayer is present, we speculate that the top layer of graphene grown on SiC(0001) in this study may already possess a level of defects comparable to that measured by TEM post-ALD. As a result, we can only definitively conclude that Ta_2O_5 results in a significant increase in the defect density of epitaxial graphene following deposition of the Ta seed layer. This claim is further supported by recent work on

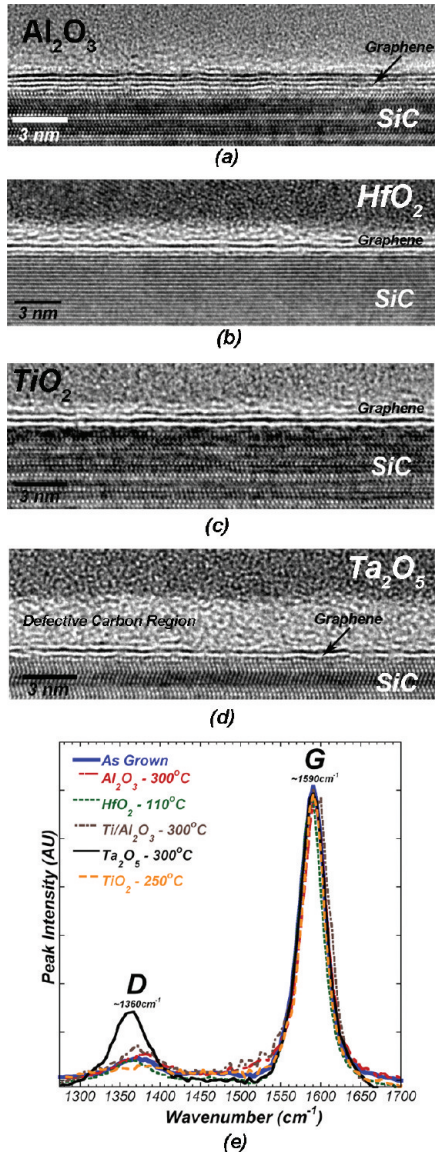

Figure 3. Deposition of dielectric materials on graphene can result in structural degradation of the underlying graphene layers. Transmission electron microscopy of (a) Al_2O_3, (b) HfO_2, (c) TiO_2, and (d) Ta_2O_5 indicates the presence of a defective top layer accompanied by an increase in the Raman D peak. Raman spectroscopy (e) confirms that Al_2O_3, HfO_2, and TiO_2 introduce only a small amount of disorder; however, the deposition of Ta_2O_5 appears to significantly degrade the quality of the underlying graphene.

exfoliated graphene transistors that utilize a seeded deposition of Al_2O_3 for the gate dielectric.[10] We do not believe the reported results would have been possible if the Al seed layer introduced a high density of defects upon seed oxidation.

Deposition of dielectric materials *via* ALD impacts the carrier mobility of epitaxial graphene. Table 1 summarizes the Lehighton mobility values at each processing step,[30] absolute change in mobility ($\Delta\mu$), and Raman D/G ratio following ALD. Lehighton mobility (a noncontact method of measuring mobility and sheet resistance) correlates well with Hall mobility in mature materials systems exhibiting a two-dimensional electron gas (*e.g.*, gallium arsenide, gallium nitride)[30] and is used here to evaluate relative changes in the graphene mobility over large areas. The majority of the samples exhibit a room temperature Lehighton mobility of approximately 1000−1300 $cm^2/(V \cdot s)$ prior to undergoing nucleation layer deposition, oxidation, and dielectric deposition. For comparison, the mobility of as-grown graphene exposed to water vapor pulses at 100 °C (oxidation step) degrades by 15%, with an increase in the D/G ratio by 1.7×. Similarly, we find that the electron-beam evaporation of a thin Al and Ta nucleation layer on graphene results in degradation of the Lehighton carrier mobility by as much as 25%, in agreement with Farmer *et al.*,[11] who report a 40% reduction in mobility following the use of an Al seed layer. The utilization of HfO_2 deposited at 110 °C without a nucleation layer provides a dielectric/graphene interface that does not significantly impact the carrier mobility, in agreement with Raman spectroscopy. Finally, the deposition of a Ti nucleation layer appears to improve the Lehighton carrier mobility by 10%, with further processing resulting in an increase in the Lehighton carrier mobility by as much as 22%. Structural and electronic modification of graphene appears to occur primarily following deposition of the nucleation layer.

The increase in D/G and magnitude of $\Delta\mu$ is well correlated to the deposition and subsequent oxidation of the ALD seed layer. This phenomenon may be linked to a potential significant change in density and atomic volume during the metal-to-oxide transformation when the nucleation layer is exposed air. Of the nucleation layers explored in this work, the Ta to Ta_2O_5 transition exhibits the most significant change in density (>2×) and volume (>14×).[21−23,28] Likewise, we measure the largest degradation of structural and electronic properties in Ta-seeded graphene. Similarly, oxidation of aluminum results in nearly a 4-fold increase in unit cell volume, second only to Ta, which correlates with the second highest D/G ratio and reduction in mobility.[24,28] Not surprisingly, the direct deposition of HfO_2, which precludes density or volume changes upon exposure to atmosphere, does not affect the D/G ratio and results in a Lehighton mobility very similar to that of pristine epitaxial graphene. Finally, the Ti to TiO_2 transition is only accompanied by a small change in volume,[21,25,28] which not only does not degrade the graphene structural properties but surprisingly also improves the mobility of carriers in the graphene. This suggests that the deposition and oxidation of Ti metal may be mild enough to not disrupt the underlying graphene and, with additional optimization, may ultimately meet the potential of high-*k* solid-state dielectrics to reduce Coulombic scattering of charge carriers.[5] While a complete understanding of the mechanism for carrier mobility improvement is not fully understood, we note that, upon deposition and subsequent oxidation of the Ti seed layer, there was a noted reduction in the carrier

TABLE 1. Summary of Lehighton Mobility (μ) Following Each Step in the Dielectric Integration Process and the Raman D/G Peak Ratio Following ALD[a]

		Lehighton mobility (μ) (±50 cm²/(V · s))					Raman
dielectric materials	deposition temp (°C)	as-grown	seed deposition	seed oxidation	dielectric deposition	post-ALD Δμ	post-processing D/G ratio
as-grown		1050				0	0.07
oxidation only	100	968		817		−151	0.12
Al_2O_3	300	978	722	776	737	−241	0.11
HfO_2	110	1300			1400	100	0.08
Ta_2O_5	300	1240	930	970	1031	−209	0.17
Ta_2O_5	150	1160	854	866	879	−281	0.25
TiO_2	120	1263	1367	1371	1520	257	0.08
TiO2	250	1372	1390	1541	1677	305	0.07
Ti seed/Al_2O_3	300	1185	1325	1380	1100	−85	0.09

[a]The impact on Lehighton mobility ranges from −25 to +22% and depends on the choice of dielectric material. Noticeably, the Lehighton mobility is most heavily affected following deposition of the nucleation layer.

concentration (~2×) as measured in Lehighton. This suggests that the TiO_2 may compensate[26] for some of the substrate doping that is known to occur in epitaxial graphene grown on SiC(0001). We also note that, while the density and volume changes discussed above are for crystalline forms of Al, Al_2O_3, Ti, TiO_2, Ta, and Ta_2O_5, the transformation from a thin, polycrystalline, metallic film to an amorphous metal-oxide film will still result in molecular density and atomic volume changes that may induce mechanical strain at the oxide/graphene interface.

The development of high-*k* gate dielectric stacks may result in superior graphene transistor performance. To date, graphene transistors have utilized SiO_2, Al_2O_3, and HfO_2 as a gate dielectrics with mixed results. Data suggest that the use of high-*k* materials such as Al_2O_3 and HfO_2 provides superior performance compared to SiO_2,[9−11] but little work has been published on the true nature of the graphene/dielectric interaction. We have shown that the use of TiO_2 could potentially improve transistor gate performance even further by minimizing extrinsic scattering centers and providing a barrier to Coulombic charge scattering. However, we note that previous work utilizing TiO_2 as a high-*k* dielectric for silicon-based and silicon-carbide-based transistors often resulted in unacceptably high gate leakage during device operation.[1,2,27] While this work does not focus on optimization of gate stacks for transistor performance, we present limited Raman and Lehighton data (Figure 3e and Table 1) of an oxidized Ti seed/Al_2O_3 gate stack that indicates the use of a Ti nucleation layer prior to Al_2O_3 (or other oxide) deposition may minimize degradation of the underlying graphene and provide superior gate dielectric for high-speed graphene transistors. Additional work is currently underway to examine the use of multilayer stacks in graphene transistors.

CONCLUSIONS

We have shown that the impact of materials integration on the structural and electronic properties of epitaxial graphene can vary widely based on the choice of dielectric material and the processing conditions used for film deposition. The depositions of Al_2O_3, HfO_2, and TiO_2 are shown to introduce minimal degradation of the epitaxial graphene structural properties, while Ta_2O_5 can significantly degrade the graphene structural quality. Furthermore, the deposition of an oxidized Ti nucleation layer prior to ALD appears to minimize the impact on the carrier mobility as measured by Lehighton and may be a good candidate as a high-*k* nucleation layer. Finally, the work presented here serves as the building block for dielectric gate stack engineering that may provide superior transistor performance in radio frequency applications.

METHODS

Graphene samples were prepared using an *in situ* hydrogen (H_2) etch, followed by Si sublimation from the Si face of semi-insulating 6H-SiC (II−VI, Inc.).[28] The *in situ* H_2 etch was performed by heating the sample to 1600 °C in 5% H_2/Ar mixture at 600 Torr and holding at 1600 °C for 60 min. Following the etch step, the chamber was cooled to 1050 °C under the H_2/Ar atmosphere and the cycle purged between 1×10^{-6} and 1 Torr with Ar to remove the H_2. Subsequently, the temperature was ramped to 1600 °C under 600 Torr Ar atmosphere to prepare for graphitization. When the growth temperature was reached, the pressure was quickly reduced to 1 Torr and held for 15 min for graphitization. Following graphitization, the pressure was returned to 600 Torr and the furnace was cooled to room temperature. Graphene films grown under these conditions are primarily one- to three-layers thick according to Raman spectroscopy and transmission electron microscopy,[29] with a D/G peak ratio of 0.07 ± 0.03.

Atomic layer deposition of Al_2O_3, HfO_2, Ta_2O_5, and TiO_2 was performed in a Cambridge Nanotech, Inc. "Savannah" ALD system.[28] Two sets of graphene samples were prepared for deposition. The first set received only an organic degrease (acetone, methanol, and deionized water wash) prior to ALD. The second set was loaded into an e-beam evaporation chamber and pumped to 1×10^{-6} Torr, after which 2 nm of the appropriate metal was deposited. Atomic layer deposition was accomplished in the following manner: (1) seed oxidation (10 s pulse of H_2O, 30 s wait, 10 cycles, 100 °C); (2) oxide deposition. Each oxide deposition requires a pulse of water followed by a wait period,

then a pulse of the correct precursor followed by another wait period. The necessary pulses and wait periods are material- and temperature-specific and happen according to a set number of cycles. Oxidation states and surface morphology of the seed layers were assessed using X-ray photoelectron spectroscopy and atomic force microscopy, respectively. The dielectric/graphene interface was characterized using a JEOL 2010F transmission electron microscope. Carrier mobility and graphene sheet resistance was evaluated with a Lehighton noncontact mobility measurement system (LEI 1605).[30] The spot size of the LEI 1605 limits the sample to $>10 \times 10$ mm^2, thus we utilize 15×15 mm^2 samples in this study and measure an average mobility of the entire sample following each processing step. X-ray photoelectron spectroscopy (XPS) confirmed complete oxidation of Al and Ta nucleation layers' exposure to atmosphere. However, Ti nucleation layers contain a combination of TiO_2, TiO, Ti_2O_3, and metallic Ti.[28] To promote full oxidation of the Ti nucleation layer, samples were exposed to a series of 10 s pulses of water vapor at 100 °C. Consequently, all graphene samples with a thin, metallic nucleation layer in this study undergo *in situ* oxidation prior to dielectric deposition.

Acknowledgment. This work was supported by the Naval Surface Warfare Center Crane, Contract No. N00164-09-C-GR34. Additionally, support for the Cambridge ALD System, WiteC Raman system, and JEOL 2010F TEM was provided by the National Nanotechnology Infrastructure Network at Penn State.

Supporting Information Available: Additional experimental details. This material is available free of charge *via* the Internet at http://pubs.acs.org.

REFERENCES AND NOTES

1. Wilk, G. D.; Wallace, R. M.; Anthony, J. M. High-*k* Gate Dielectrics: Current Status and Material Properties Considerations. *J. Appl. Phys.* **2001**, *89*, 5243–5275.
2. Robertson, J. High Dielectric Constant Gate Oxides for Metal Oxide Si Transistors. *Rep. Prog. Phys.* **2006**, *69*, 327–396.
3. Jang, C.; Adam, S.; Chen, J. H.; Williams, E. D.; Das, S.; Fuhrer, M. S. Tuning the Effective Fine Structure Constant in Graphene: Opposing Effects of Dielectric Screening on Short- and Long-Range Potential Scattering. *Phys. Rev. Lett.* **2008**, *101*, 146805.
4. Chen, F.; Xia, J.; Tao, N. Ionic Screening of Charged-Impurity Scattering in Graphene. *Nano Lett.* **2009**, *9*, 1621–1625.
5. Chen, F.; Xia, J.; Ferry, D.; Tao, N. Dielectric Screening Enhanced Performance in Graphene FET. *Nano Lett.* **2009**, *9*, 2571–2574.
6. Konar, A.; Fang, T.; Jena, D. Effect of High-K Dielectrics on Charge Transport in Graphene. Preprint at arXiv:0902.0819v1 [cond-mat.mtrl-sci].
7. Ponomarenko, L. A.; Yang, R.; Mohiuddin, T. M.; Katsnelson, M. I.; Novoselov, K. S.; Morozov, S. V.; Zhukov, A. A.; Schedin, F.; Hill, E. W.; Geim, A. K. Effect of a High-κ Environment on Charge Carrier Mobility in Graphene. *Phys. Rev. Lett.* **2009**, *102*, 206603.
8. Williams, J. R.; DiCarlo, L.; Marcus, C. M. Quantum Hall Effect in a Gate-Controlled p−n Junction of Graphene. *Science* **2007**, *317*, 638.
9. Lemme, M. C.; Echtermeyer, T. J.; Baus, M.; Kurz, H. A Graphene Field-Effect Device. *IEEE Electron Device Lett.* **2007**, *28*, 282.
10. Kim, S.; Nah, J.; Jo, I.; Shahrjerdi, D.; Colombo, L.; Yao, Z.; Tutuc, E.; Banerjee, S. Realization of a High Mobility Dual-Gated Graphene Field-Effect Transistor with Al_2O_3 Dielectric. *Appl. Phys. Lett.* **2009**, *94*, 062107.
11. Farmer, D.; Chiu, H. Y.; Lin, Y. M.; Jenkins, K.; Xia, F.; Avouris, P. Utilization of a Buffered Dielectric to Achieve High Field-Effect Carrier Mobility in Graphene Transistors. *Nano Lett.* **2009**, *9*, 4474–4478.
12. Lee, B.; Park, S. Y.; Kim, H. C.; Cho, K. J.; Vogel, E. M.; Kim, M. J.; Wallace, R. M.; Kim, J. Conformal Al_2O_3 Dielectric Layer Deposited by Atomic Layer Deposition for Graphene-Based Nanoelectronics. *Appl. Phys. Lett.* **2008**, *92*, 203102.
13. Lin, Y. M.; Jenkins, K. A.; Valdes-Garcia, A.; Small, J. P.; Farmer, D. B.; Avouris, P. Operation of Graphene Transistors at Gigahertz Frequencies. *Nano Lett.* **2009**, *9*, 422.
14. Wang, X.; Tabakman, S. M.; Dai, H. Atomic Layer Deposition of Metal Oxides on Pristine and Functionalized Graphene. *J. Am. Chem. Soc.* **2008**, *130*, 8152.
15. Moon, J. S.; Curtis, D.; Hu, M.; Wong, D.; McGuire, C.; Campbell, P. M.; Jernigan, G.; Tedesco, J.; VanMil, B; Myers-Ward, R.; Eddy, C; Gaskill, D. Epitaxial-Graphene RF Field-Effect Transistors on Si-Face 6H-SiC Substrates. *IEEE Electron Device Lett.* **2009**, *30*, 650–652.
16. Prinkle, A.; Wallace, R.; Colombo, L. *In Situ* Studies of Al_2O_3 and HfO_2 Dielectrics on Graphite. *Appl. Phys. Lett.* **2009**, *95*, 133106.
17. Zou, K.; Hong, X; Keefer, D; Zhu, J. The Deposition of High-Quality HfO_2 on Graphene and the Effect of Remote Oxide Phonon Scattering. Preprint at arXiv:0912.1378v2 [cond-mat.mtrl-sci].
18. Avouris, P. Graphene Electronics and Optoelectronics. AVS 56th International Symposium & Exhibition 2009, Graphene Topical Conference, GR+TF-TuA7.
19. Cancado, L. G.; Takai, K.; Enoki, T.; Endo, M.; Kim, Y. A.; Mizusaki, H.; Jorio, A.; Coelho, L. N.; Magalhaes-Paniago, R; Pimenta, M. General Equation for the Determination of the Crystallite Size L_a of Nanographite by Raman Spectroscopy. *Appl. Phys. Lett.* **2006**, *88*, 163106.
20. Robinson, J. A.; Weng, X.; Trumbull, K.; Cavalero, K.; Wetherington, M.; Frantz, E.; LaBella, M.; Hughes, Z.; Fanton, M.; Snyder, D. Nucleation of Epitaxial Graphene on SiC(0001). *ACS Nano* **2010**, *4*, 153–158.
21. McCallister, W. C. *Materials Science and Engineering: An Introduction*; Wiley: New York.
22. Steidel, C. A.; Gerstenberg, D. Thermal Oxidation of Sputtered Tantalum Thin Films between 100° and 525 °C. *J. Appl. Phys.* **1969**, *40*, 3828–3835.
23. *PCPDFWIN*, version 2.01; Card# 04-0788, 25-0922, and 27-1447; International Centre for Diffraction Data, 1998.
24. *PCPDFWIN*, version 2.01; Card# 44-1294 and #82-0514; International Centre for Diffraction Data, 1998.
25. *PCPDFWIN*, version 2.01; Card# 04-0787 and #83-2081; International Centre for Diffraction Data, 1998.
26. While Lehighton measurements correlate well with Hall mobility for GaAs and GaN, we note that validation of the Lehighton measurements for mobility, sheet resistance, and carrier concentration is warranted to ensure that TiO_2 does in fact act as a compensating layer. As a result, we are currently fabricating and testing structures to extract the true Hall mobility.
27. Mahapatra, R.; Chakraborty, A. K.; Poolamai, N.; Horsfall, A.; Chattopadhyay, S.; Wright, N. G.; Coleman, K.; Coleman, P. G.; Burrows, C. P. Leakage Current and Charge Trapping Behavior in TiO_2/SiO_2 High-Gate Dielectric Stack on 4H-SiC Substrate. *J. Vac. Sci. Technol., B* **2007**, *25*, 217–223.
28. Refer to online Supporting Information for additional information.
29. Röhrl, J.; Hundhausen, M.; Emtsev, K. V.; Seyller, T.; Graupner, R.; Ley, L. Raman Spectra of Epitaxial Graphene on SiC(0001). *Appl. Phys. Lett.* **2008**, *92*, 201918.
30. Nguyen, D.; Hogan, K.; Blew, A.; Cordes, M. Improved Process Control, Lowered Costs and Reduced Risks through the Use of Non-destructive Mobility and Sheet Carrier Density Measurements on GaAs and GaN Wafers. *J. Cryst. Growth* **2004**, *272*, 59–64.